Structure of d(GCGAAAGC) (hexagonal form): a base-intercalated duplex as a stable structure

Tomoko Sunami,[a] Jiro Kondo,[a] Ichiro Hirao,[b,c] Kimitsuna Watanabe,[d] Kin-ichiro Miura[e] and Akio Takénaka[a]*

[a]Graduate School of Bioscience and Biotechnology, Tokyo Institute of Technology, Yokohama 226-8501, Japan, [b]RIKEN GSC, Wako-shi, Saitama 351-0198, Japan, [c]Research Center for Advanced Science and Technology, University of Tokyo, Tokyo 153-8904, Japan, [d]Graduate School of Engineering, University of Tokyo, Tokyo 113-8656, Japan, and [e]Faculty of Science, Gakushuin University, Tokyo 171-8588, Japan

Correspondence e-mail:
atakenak@bio.titech.ac.jp

A DNA fragment d(GCGAAAGC), postulated to adopt a stable mini-hairpin structure on the basis of its extraordinary properties, has been X-ray analyzed. Two octamers related by a crystallographic twofold symmetry are aligned in an antiparallel fashion and associate to form a duplex, which is maintained by two Watson–Crick G·C base pairs and a subsequent sheared G·A pair at both ends. The central two A residues are free from base-pair formation. The corresponding base moieties of the two strands are intercalated and stacked on each other, forming a long column of G_1-C_2-G_3-A_4-A_5^*-A_5-A_4^*-G_3^*-C_2^*-G_1^* (asterisks indicate the counter-strand). The Watson–Crick and major-groove sites of the four stacked adenine bases are exposed to the solvent region, suggesting a functional role. Since this structural motif is similar to those found in the nonamers $d(G^{Br}CGAAAGCT)$ and $d(G^ICGAAAGCT)$, the base-intercalated duplex may be a stable form of the specific sequence. Electrophoresis results suggest that the octamer has two states, monomeric and dimeric, in solution depending on the Mg^{2+} concentration. The present duplex is preferred under the crystallization conditions, which correspond to physiologically allowed conditions.

1. Introduction

DNA is a highly sophisticated chemically stable medium for the storage of genetic information that is able to adopt a duplex form, with redundant information encoded through the complementary base–base interactions. In contrast, RNA generally exists as a single strand but is folded into a complicated three-dimensional structure, so that it serves as a functional molecule similar to proteins. Typical examples are found in ribosomal RNAs (Harms *et al.*, 2001; Ban *et al.*, 2000; Yusupov *et al.*, 2001; Wimberly *et al.*, 2000), hammerhead ribozymes (Pley *et al.*, 1994; Scott *et al.*, 1995), hairpin ribozyme (Rupert & Ferre-D'Amare, 2001) and group I intron ribozymes (Cate *et al.*, 1996), in which stems composed of two antiparallel strands are folded into a globular form by tertiary interactions involving loops and bulges.

In living cells, it is difficult to find a functional DNA similar to RNA, because every organism has been established and has evolved on the basis of the complementary system of DNA. Recent *in vitro* selection techniques, however, have made it possible to create a functional DNA which catalyzes an RNA-cleavage reaction (Breaker & Joyce, 1994). As a material for this purpose, DNA may be more useful owing to its chemical stability. Such a single-stranded DNA would adopt a specific folded structure through inter-strand and intra-strand interactions. In order to establish the structural basis for designing

Table 1
Crystal data, data-collection and structure-refinement statistics.

(*a*) Data collection.

	9hmt-I		8hmt-h
X-ray facility	Photon Factory		Photon Factory
Space group	$P6_322$		$P6_322$
Unit-cell parameters (Å)	$a = b = 36.7, c = 64.8$		$a = b = 37.4,$ $c = 64.6$
Asymmetric unit†	1		1
Temperature (K)	293	100	100
Wavelength (Å)	1.00	1.00	0.978
Resolution (Å)	29–1.8	18–1.4	32–2.1
Observed reflections	65260	546817	102876
Unique reflections	4017	5553	1817
Completeness (%)	89.4	99.9	100
Partial completeness in the outer shell (%)	74.6 (1.80–1.88 Å)	100 (1.4–1.43 Å)	100 (2.1–2.21 Å)
R_{merge}‡/R_{anom}§ (%)	5.5/3.2	6.1	4.4

(*b*) Structure refinement.

	9hmt-I	8hmt-h
Resolution range (Å)	10.0–1.4	10.0–2.15
Used reflections ($F_o > 3\sigma$)	5111	1538
R (%)¶	20.9	22.7
R_{free} (%)††	23.6	23.9
No. DNA atoms	168	164
No. water molecules	48	28
No. hexamminecobalts	1/3	1/3
No. hydrated magnesiums	1/3	1, 1/3
No. chloride ions	1/3	1/3
R.m.s deviation from ideal geometry		
Bond lengths (Å)	0.005	0.007
Bond angles (°)	0.9	1.0
Improper angles (°)	1.4	1.4

† Single-strand DNA. ‡ $R_{merge} = 100 \times \sum_{hklj} |I_{hklj} - \langle I_{hkl} \rangle| / \sum_{hklj} \langle I_h kl \rangle$. § $R_{anom} = 100 \times \sum_{hklj} |I_{hklj}(+) - I_{hklj}(-)| / \sum_{hklj} [I_{hklj}(+) + I_{hklj}(-)]$. ¶ $R = 100 \times \sum ||F_o| - |F_c|| / \sum |F_o|$, where $|F_o|$ and $|F_c|$ are the observed and calculated structure-factor amplitudes, respectively. †† Calculated using a random set containing 10% of observations that were not included during refinement (Brünger *et al.*, 1998).

such molecules, it is necessary to investigate the structural features of single-stranded DNA.

It was found that DNA fragments containing the sequence d(GCGAAAGC) exhibit extraordinary properties, with (i) abnormal mobility in electrophoresis (Hirao *et al.*, 1988), (ii) high thermostability (Hirao *et al.*, 1989), (iii) unusual CD spectra (Hirao *et al.*, 1989) and (iv) robustness against nuclease digestion (Hirao *et al.*, 1992). To explain these properties, a mini-hairpin structure was postulated. X-ray analyses of oligonucleotides containing the sequence d(GCGAAAGC) were initiated in order to reveal their structural features. In the crystal of the nonamer d(GCGAAAGCT) (Sunami *et al.*, 2002), the four 5′-end residues with sequence d(CGAA) form a parallel duplex with those of another nonamer through homo base-pair formations. The remaining four residues d(AGCT) form an antiparallel duplex with those of another parallel duplex. This is quite different from the mini-hairpin structure. We found that an iodo-derivative of the nonamer, d(G^{I}CGAAAGCT), crystallized in a different habit which is rather similar to that of the octamer d(GCGAAAGC). To investigate the underlying structural versatility, X-ray analyses of these two DNA fragments were performed.

2. Materials and methods

2.1. Synthesis, crystallization and data collection

DNA oligomers with sequences d(G^{I}CGAAAGCT) (subsequently abbreviated 9hmt-I) and d(GCGAAAGC) (subsequently 8hmt-h) were synthesized on a DNA synthesizer and purified by HPLC and gel filtration. Crystallization conditions for 9hmt-I were surveyed at 293 K using the hanging-drop vapour-diffusion method. A droplet was prepared by mixing 2 µl of a 2 m*M* DNA solution containing 9 m*M* 2,6-diaminopyridine[1] and 2 µl of a reservoir solution containing 20 m*M* MgCl$_2$, 80 m*M* NaCl, 30 m*M* Co(NH$_3$)$_6$Cl$_3$, 20% 2-methyl-2,4-pentanediol and 0.17% *n*-decanoyl-*N*-methylglucamide (purchased from Dojindo Laboratories Co. Ltd) in 40 m*M* sodium cacodylate buffer pH 6.0. When the droplet was equilibrated with the reservoir solution, hexagonal crystals grew to 200×150 µm in size within a few days. Crystals of 8hmt-h (150×25 µm in size) were obtained at 277 K: a droplet prepared by mixing 2 µl of a 1.5 m*M* DNA solution and 2 µl of 50 m*M* sodium cacodylate buffer pH 7.0 containing 18 m*M* MgCl$_2$, 2.25 m*M* spermine.4HCl, 0.9 m*M* Co(NH$_3$)$_6$Cl$_3$ and 4.5% 2-methyl-2,4-pentanediol was equilibrated with 25% 2-methyl-2,4-pentanediol for 10 d. Suitable crystals for X-ray analysis were mounted in nylon cryoloops (Hampton Research) and stored in liquid nitrogen.

For phase determination, X-ray data from 9hmt-I were collected at room temperature using the Weissenberg method (Sakabe, 1991) at BL6A of Photon Factory (PF; λ = 1.00 Å), Tsukuba. A suitable crystal was sealed in a glass capillary and X-ray diffraction was recorded on imaging plates positioned 429.7 mm from the crystal. At first, each frame was taken using an 11.1° oscillation with a coupling constant of 1.5° mm^{-1} and an exposure time of 110 s. Using the same crystal, a second data set was obtained using a 17.5° oscillation with a coupling constant of 1.7° mm^{-1} and an exposure time of 35 s, in order to compensate for overloaded reflections. The third data set was obtained using an 11.4° oscillation, a 2° mm^{-1} coupling constant and a 456 s exposure time using another crystal. These diffraction patterns were processed with the program *DENZO* (Otwinowski & Minor, 1997). The three data sets were scaled and merged at 1.8 Å resolution using the programs *SCALA*, *AGROVATA* and *TRUNCATE* from the *CCP*4 suite (Collaborative Computational Project, Number 4, 1994).

For structure refinement, a further data set was collected at 100 K with synchrotron radiation (λ = 1.00 Å) at PF. X-ray data were recorded on a CCD detector (Quantum 4R) positioned at 80 mm from the crystal. Three data sets were collected with 1° oscillations for 120, 50 and 5 s exposure times and then processed at 1.4 Å resolution using the program *DPS*/*MOSFLM* (Leslie, 1992; Steller *et al.*, 1997; Rossmann & van Beek, 1999; Powell, 1999). The intensity data were scaled and merged using the programs *SCALA* and *TRUNCATE* from the *CCP*4 suite.

---

[1] Similar crystals can be obtained without 2,6-diaminopyridine.

research papers

At 100 K, X-ray diffraction from 8hmt-h was recorded on a CCD detector (Quantum 4R) positioned at a distance of 150 mm at PF beamline 18B ($\lambda = 0.978$ Å). Two data sets were collected using 1° oscillations for 40 and 6 s exposure times. The diffraction images were processed at 2.1 Å resolution.

Data-collection statistics and crystal data of the two crystals are given in Table 1. The 9hmt-I and 8hmt-h crystals are isomorphous, the space group being the same ($P6_322$) with similar unit-cell parameters ($a = b = 36.7$, $c = 64.8$ Å for 9hmt-I; $a = b = 37.4$, $c = 64.6$ Å for 8hmt-h). R_{merge} for 9hmt-I is 6.1% for 5553 independent reflections and R_{merge} for 8 hmt-h is 4.4% for 1817 independent reflections.

2.2. Structure determination and refinement

The I-atom position in the 9hmt-I crystal was determined from an anomalous difference Patterson map calculated using the room-temperature data set. The remaining structure, except for the ninth T residue, was constructed from successive Fourier maps initially derived by the heavy-atom method[2] using the program *QUANTA* (Molecular Simulation Inc.). It was difficult to distinguish between the two possible structures, hairpin dimer and duplex dimer, because the density of the A_5 residue was rather poor and the structures both looked reasonable. To resolve this situation, the atomic parameters were refined for both models using the higher resolution data measured at low temperature. The computer program *CNS* (Brünger *et al.*, 1998) was used to perform a combination of rigid-body, simulated-annealing, crystallographic conjugate-gradient minimization refinement and *B*-factor refinement, followed by interpretation of omit maps at every nucleotide residue. The refined electron-density maps clearly indicated that the duplex dimer was correct, as did the *R* values. A

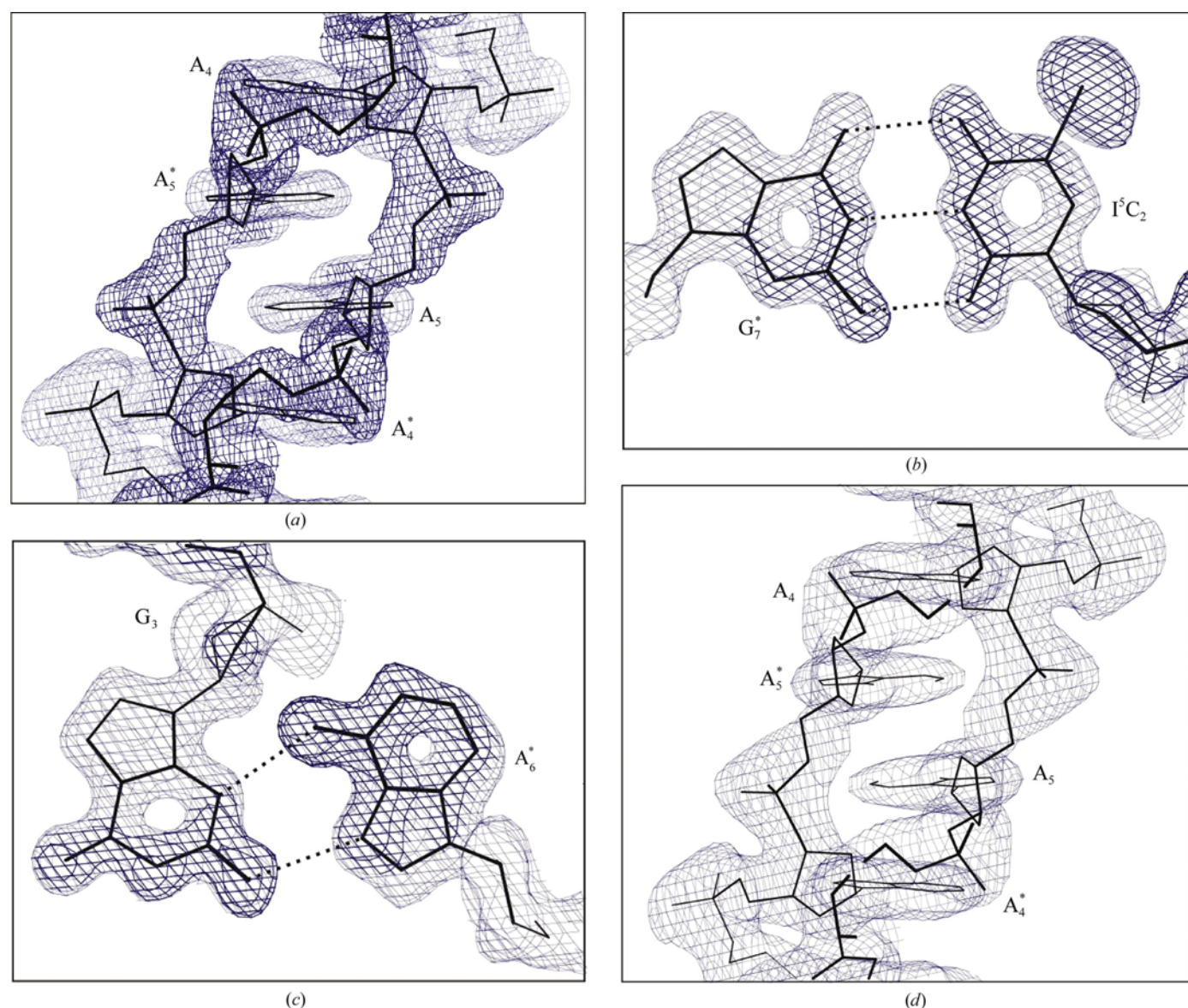[2] Initially solved in 1997, prior to the publication by Shepard *et al.* (1998).

Figure 1
Local $2F_o - F_c$ maps for 9hmt-I (*a*, *b*, *c*) and 8hmt-h (*d*). Densities are contoured at the 1σ level. Broken lines indicate possible hydrogen bonds.

hexamminecobalt cation, a hydrated magnesium cation, a chloride ion and 48 water molecules appeared in the $F_o - F_c$ map and were included in the final refinements. No restraints were applied to base–base interactions and sugar puckers. The final $2F_o - F_c$ map showed that the central A_5 residue has a relatively high flexibility and that the 3'-terminal thymidine residue is disordered in the solvent region.

Since the two crystals of 9hmt-I and 8hmt-h were apparently isomorphous, the structure of the latter crystal was determined by the molecular-replacement method (using the program *AMoRe*; Navaza, 1994) using the 9hmt-I structure except for the terminal T residue. The atomic parameters were then refined in a manner similar to that for 9hmt-I using the program *CNS* (Brünger *et al.*, 1998). In this case the hairpin dimer was also examined, but the electron-density map clearly indicated that the duplex dimer was correct. A hexamminecobalt cation, two hydrated magnesium cations, a chloride ion and 28 water molecules were included in the further refinements. No restraints were applied to base–base interactions and sugar puckers.

Structure-refinement statistics are summarized in Table 1. The final $2F_o - F_c$ map is shown in Fig. 1, drawn with the program *O* (Jones *et al.*, 1991). All local helical parameters, including torsion angles and the pseudorotation phase angles of ribose rings, were calculated using the program *3DNA* (Lu & Olson, 2003). Pictures of the structures were drawn with the programs *MOLSCRIPT* (Kraulis, 1991) and *RASMOL* (Sayle & Milner-White, 1995).

2.3. Electrophoresis experiments

To compare the structural composition in solution and in the crystalline state, native PAGE was performed at room temperature for 8hmt in solution and for its redissolved crystals. Gels were prepared from a 89 mM Tris borate and 2 mM EDTA buffer solution containing 19% acrylamide, 1% N,N'-methylenebis(acrylamide) and a small amount of ammonium oxodisulfate and N,N,N',N'-tetramethylethylenediamine. A glycerol solution containing xylene cyanol and bromophenol blue was used for loading. Washed crystals were dissolved in 1.5 µl loading buffer. Gels were dyed with toluidine blue. To examine the Mg^{2+}-ion dependency of the structure, native PAGE was performed at room temperature using a buffer solution containing 100 mM Tris borate, 20 mM magnesium acetate and 20 mM sodium acetate. 8hmt samples pre-incubated at different Mg^{2+} concentrations were loaded. Gels were dyed with Silver Strain II Kit Wako (purchased from Wako Pure Chemical Industries Ltd).

3. Results and discussion

In the crystal of 8hmt-h, the two octamers related by crystallographic twofold symmetry are aligned in an antiparallel fashion and associated with each other to form a duplex, as shown in Fig. 2.[3] Therefore, each half of the duplex is crystallographically independent. At both ends of the duplex, two Watson–Crick G·C base pairs $G_1 \cdot C_8^*$ and $C_2 \cdot G_7^*$ or $C_8 \cdot G_1^*$ and $G_7 \cdot C_2^*$ are formed (see Fig. 3). The subsequent G_3 residue forms a sheared pair with the A_6 residue of the counter strand, $G_3 \cdot A_6^*$ or $A_6 \cdot G_3^*$, as shown in Fig. 3, through the two hydrogen bonds, N2H···N7 and N3···HN6. An additional hydrogen bond O4'···HN6 supports the base-pair formation. It is interesting to note that the remaining two residues, A_4 and A_5,

---

[3] To describe the detailed structures, the following numbering schemes are subsequently employed for nucleotide residues and atoms: X_n: is the nth residue X and Xn is the nth atom X according to the IUPAC–IUPAB nomenclature.
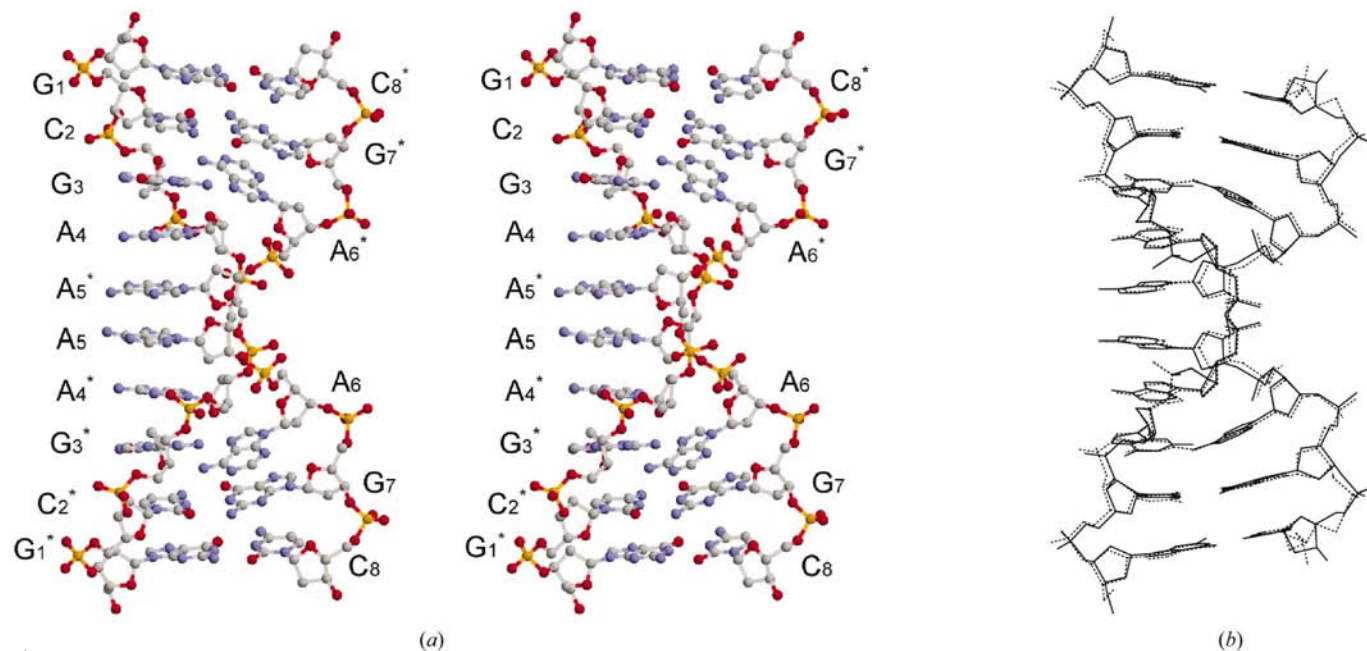

Figure 2
A stereo-pair diagram of the base-intercalated duplex of 8hmt-h (*a*) and a superimposition of the two structures of 8hmt-h (full line) and 9hmt-I (broken line) (*b*). The 3'-terminal T_9 residues are omitted owing to their disorder. * indicates the counter-strand aligned in antiparallel fashion.

are not involved in base-pair formation. Their base moieties are respectively stacked on those of the other strand, so that A_5 is intercalated between A_4^* and A_5^* and A_5^* is intercalated between A_4 and A_5 (see Fig. 4). These four adenine bases, A_4, A_5^*, A_5 and A_4^*, expose their Watson–Crick and major-groove sites[4] into the solvent region to interact with the surrounding water molecules. The central A_5 residue is relatively flexible with high temperature factors. There are three different stacked columns in a duplex. A long column of G_1-C_2-G_3-A_4-A_5^*-A_5-A_4^*-G_3^*-C_2^*-G_1^* is formed by base-intercalation of the two strands. Two short columns, A_6-G_7-C_8 and A_6^*-G_7^*-C_8^*, occur in the respective strands.

In the crystal, an extended column is formed along the c axis by stacking interactions between the $G_1 \cdot C_8^*$ pairs of the two duplexes related by the crystallographic twofold symmetry (Fig. 5). Among the three extended columns, the duplexes are bound to a hexamminecobalt cation located on the crystallographic threefold axis, the bound ammonia molecules being hydrogen bonded to the O6 and N7 atoms in the major-groove

---

[4] 'Watson–Crick sites' mean the donor and the acceptor sites for the hydrogen bonds forming the Watson–Crick base pairs.

sites of the three G_3 residues (Fig. 6). A hydrated magnesium cation is bound to the major-groove site of the G_7 residue.

In the 9hmt-I crystal, the first eight residues form a duplex, similar to that of 8hmt-h, with an r.m.s. deviation of 0.5 Å when they are superimposed on each other (see Fig. 2b). Therefore, the I atom introduced at the second residue of 9hmt-I has no significant steric effect on the duplex conformation. These structural features of 8hmt-h and 9hmt-I are similar to those of a duplex reported for the bromo-derivative d(G^{Br}CGAAAGCT) (subsequently referred to as 9hmt-Br; Shepard *et al.*, 1998). The r.m.s. deviation between the two halogeno derivatives is 0.8 Å. The 3′-terminal T residue, except for its 5′-phosphate group, is disordered in a large solvent tunnel around the crystallographic threefold axis, similar to the bromo derivative.

The helical parameters and sugar puckers are given in Table 2. In the stem regions, the G_1, C_2 and G_7 residues adopt a C2′-*endo* pucker to form the canonical B-form conformation. At the third residue, the C1′—C1′ distance becomes shorter and the twist angle larger to form the sheared pair between the minor-groove site of the G_3 residue and the major-groove site of the A_6 residue. However, the two residues adopt a C2′-*endo* conformation. To support the base-intercalated stacking of successive A residues, the G·A pairs serve as the scaffold. The A_4 and A_5 residues adopt C3′-*endo* and C2′-*endo* puckers, respectively. The C3′-*endo* pucker is required to make an open space for intercalation of the A_5^* adenine bases between the A_4 and A_5 residues. Other conformational differences are found in the torsion angles around the P—O5′ and C5′—C4′ bonds of the A_5 residue, the
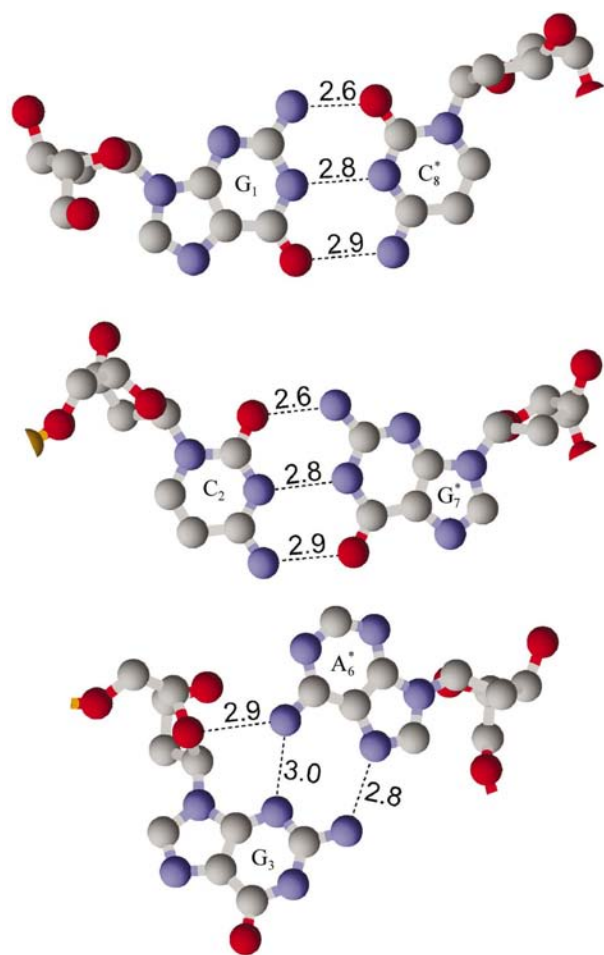

Figure 3
The three independent base pairs which form the stems at both ends of the base-intercalated duplex of 8hmt-h. Values indicate the hydrogen-bond distances in Å.
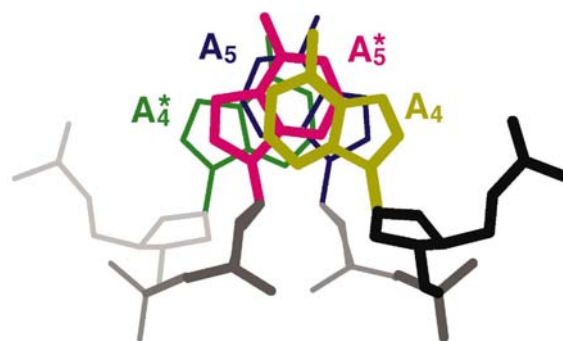

Figure 4
Four adenine bases stacked in the central part of the base-intercalated duplex of 8hmt-h.
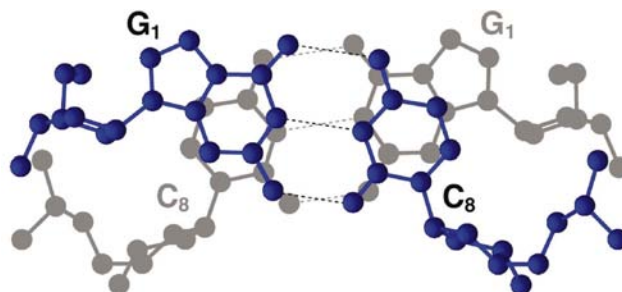

Figure 5
Two G·C pairs stacked between the ends of the base-intercalated duplexes.

Table 2
Some helical parameters and sugar puckers of the base-intercalated duplexes.

Inclin, Prop, Buckl and Open represent inclination, propeller twist, buckle and opening angles (see Lu & Olson, 2003). The C_2 residue is iodinated in 9hmt-I and brominated in 9hmt-Br. For each base pair, the upper line is for 9hmt-I, the middle line for 8hmt-h and the lower line for 9hmt-Br (Shepard *et al.*, 1998). The corresponding values for the remaining half of the duplex are omitted owing to crystallographic symmetry.

(*a*) Helical parameters.

Base pair	Inclin	Tip	Twist	dz	Prop	Buckl	Open	C1′···C1′
$G_1 \cdot C_8^*$	1	−6	26	3.1	6	−2	−3	10.7
	−2	−8	28	3.0	9	0	3	10.5
	2	3	31	3.2	6	−1	1	10.5
$C_2 : G_7^*$	6	0	55	3.3	10	13	0	10.5
	10	3	52	3.2	4	16	1	10.5
	10	0	52	3.4	8	9	−1	10.6
$G_3 : A_6^*$	†	†	†	†	−12	29	9	8.3
	†	†	†	†	−4	31	8	8.4
	†	†	†	†	−15	25	10	8.5
A form	20	0	33	2.3	12	0	−2	10.7
B form	−5	0	36	3.4	−1	0	−2	10.7

(*b*) Sugar puckers.

Nucleotide	Pucker, 9hmt-I	Pucker, 8hmt-h	Pucker, 9hmt-Br
G_1	C3′-*exo*	C3′-*exo*	C3′-*exo*
C_2	C1′-*exo*	C1′-*exo*	C1′-*exo*
G_3	C2′-*endo*	C2′-*endo*	C2′-*endo*
A_4	C3′-*endo*	C3′-*endo*	C4′-*exo*
A_5	C1′-*exo*	C3′-*endo*	C1′-*exo*
A_6	C2′-*endo*	C2′-*endo*	C2′-*endo*
G_7	C1′-*exo*	C1′-*exo*	C2′-*endo*
C_8	C2′-*endo*	C4′-*exo*	C3′-*exo*
T_9	‡	‡	‡
A form	C3′-*endo*	C3′-*endo*	C3′-*endo*
B form	C2′-*endo*	C2′-*endo*	C2′-*endo*

† A_4 and A_5 are not paired with any bases. ‡ T_9 is disordered.

α and γ angles being −155 and 170°, respectively. These angles also facilitate the backbone extension.

In the duplex conformation (Table 2), the two base-intercalated structures are similar to the zipper-like duplex reported for 9hmt-Br (Shepard *et al.*, 1998), confirming that even in the iodo-derivative 9hmt-I the base-intercalated structure is preferred.[5] In addition, the present work has revealed that the octamer d(GCGAAAGC) 8hmt-h with natural nucleotides and missing the 3′-terminal T residue also adopts the same base-intercalated duplex. These results apparently indicate that the sequence d(GCGAAAGC) is specifically adapted to form a base-intercalated duplex under conditions containing Mg^{2+} ions.

From extensive solution studies, a mini-hairpin structure was postulated for the octamer as described in the introduction. In contrast, the structure in the crystalline state is quite different. It is interesting to examine further the possibility of a mini-hairpin structure. The base-intercalated structure has the following features: (i) the central A_5 residues are flexible and (ii) the duplex structure is similar to a mini-hairpin dimer.

---

[5] In this paper, we refer to the structural motif observed here as the base-intercalated duplex, to distinguish it from the base-paired duplex.

In the structure determination of 9hmt-I at 1.8 Å resolution, as electron densities for the A_5 residues were relatively broadened owing to disorder, two possible structures could be traced for the phosphate backbone chain. One was the base-intercalated duplex and the other was a mini-hairpin dimer. Changing the local phosphate-backbone conformations and the sugar pucker of the A_5 residues slightly, one can easily derive the latter structure as a reasonable alternative in which the two mini-hairpin monomers are stacked head-to-head, facing each other at the A_5 residues. However, the final electron-density map at 1.4 Å resolution definitely indicates that the structure in the crystal is the base-intercalated duplex (see Fig. 1*a*).

The first question is why the octamer exists as a base-intercalated duplex in the crystalline state and as a mini-hairpin monomer in solution. Even when the 8hmt-h crystals was dissolved, native PAGE patterns indicate the monomeric state, as shown in Figs. 7(*a*) and 7(*b*). A most remarkable difference is found on changing the salt concentration, as pointed out by Shepard *et al.* (1998) for the case of the nonamer. To examine salt effects on the tertiary structures, native PAGE experiments were performed for the octamer at different $MgCl_2$ concentrations. As shown in Fig. 7(*c*), a small weak band corresponding to a dimer appears at higher concentrations. Therefore, it can be concluded that the duplex formation of the octamer is preferred under high-salt conditions.

The second question is why the 9hmt-I structure differs from that of the native nonamer d(GCGAAAGCT) (subsequently referred to as 9hmt) in which one half of the sequence forms a parallel duplex and the remaining half forms an antiparallel duplex (Sunami *et al.*, 2002). To form such a parallel duplex, hemi-protonation at the C_2 residue is essen-
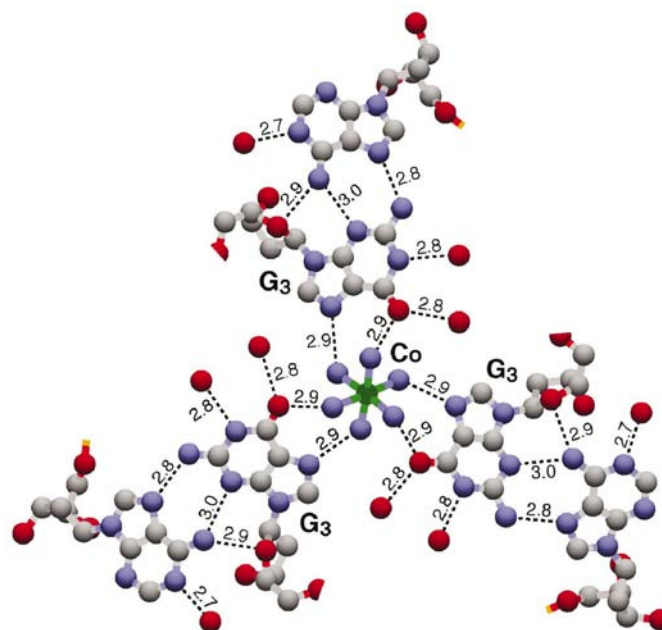
Figure 6
An assembly of three base-intercalated duplexes of 8hmt-h. A hexamminecobalt cation is bound in the major grooves of the three guanine residues.
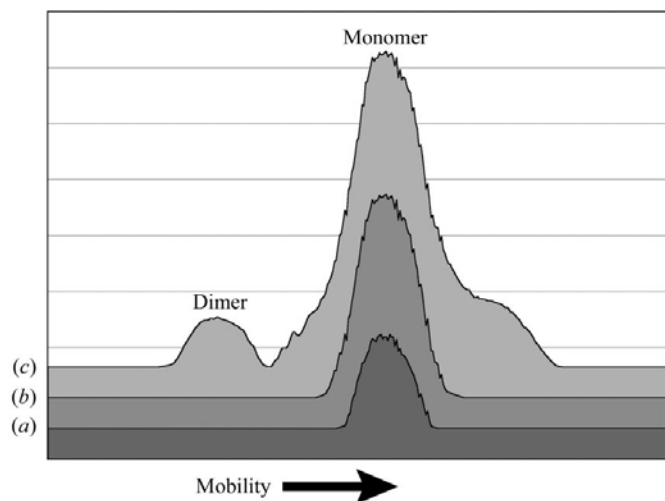
Figure 7
Scanned native PAGE patterns of 8hmt in solution (*a*), dissolved crystals (*b*) and with 20 m*M* Mg^{2+} (*c*).

tial. The hemi-protonated C:C$^+$ pair is stable in the pH range 4.7–6.8 (Robinson *et al.*, 1992; Robinson & Wang, 1993; Inman, 1964), although the pK_a value for native cytidine is around 4.5 (Albert, 1973). In contrast, the second C residue of 9hmt-I is halogenated, decreasing its acidity (the pK_a value is 3.0 for 5-iodocytidine; Albert, 1973). Therefore, 9hmt-I cannot form the 9hmt structure under its crystallization conditions (pH 6.0), but it may be able to adopt the 9hmt structure at lower pH.

The final question is whether the present structures are involved in some biological function, as the crystallization conditions used for the present crystals are physiologically acceptable, except for the hexamminecobalt cation. As the major parts of living systems are established by using the Watson–Crick pairing between complementary strands, it may be difficult to find such a unique sequence in the stable double-helix structure. However, single-stranded DNAs from DNA viruses or phages can adopt many types of structure (like RNA); the base-intercalated motif may then occur and have a specific function. For example, a sequence containing GAAA and related sequences are found in the replication origin of phage G4 (Hirao *et al.*, 1990) and in centromeres of humans and other higher eukaryotes (Grady *et al.*, 1992). Another example of single-stranded DNA is a DNA enzyme derived by *in vitro* selection (Sioud, 2001). As the base-intercalated structure is stable, it may serve as a building motif of such functional DNAs.

References

Albert, A. (1973). *Synthetic Procedures in Nucleic Acid Chemistry*, Vol. 2, edited by W. W. Zorbach & S. Tipson, pp. 1–46. New York: John Wiley & Sons.

Ban, N., Nissen, P., Hansen, J., Moore, P. B. & Steitz, T. A. (2000). *Science*, **289**, 905–920.

Breaker, R. R. & Joyce, G. F. (1994). *Chem. Biol.* **1**, 223–229.

Brünger, A. T., Adams, P. D., Clore, G. M., DeLano, W. L., Gros, P., Grosse-Kunstleve, R. W., Jiang, J.-S., Kuszewski, J., Nilges, M., Pannu, N. S., Read, R. J., Rice, L. M., Simonson, T. & Warren, G. L. (1998). *Acta Cryst.* D**54**, 905–921.

Cate, J. H., Gooding, A. R., Podell, E., Zhou, K., Golden, B. L., Kundrot, C. E., Cech, T. R. & Doudna, J. A. (1996). *Science*, **273**, 1678–1685.

Collaborative Computational Project, Number 4 (1994). *Acta Cryst.* D**50**, 760–763.

Grady, D. L., Ratliff, R. L., Robinson, D. L., McCanlies, E. C., Meyne, J. & Moyzis, R. K. (1992). *Proc. Natl Acad. Sci. USA*, **89**, 1695–1699.

Harms, J., Schluenzen, F., Zarivach, R., Bashan, A., Gat, S., Agmon, I., Bartels, H., Franceschi, F. & Yonath, A. (2001). *Cell*, **107**, 679–688.

Hirao, I., Ishida, M., Watanabe, K. & Miura, K. (1990). *Biochim. Biophys. Acta*, **1087**, 199–204.

Hirao, I., Naraoka, T., Kanamori, S., Nakamura, M. & Miura, K. (1988). *Biochem. Int.* **16**, 157–162.

Hirao, I., Nishimura, Y., Naraoka, T., Watanabe, K., Arata, Y. & Miura, K. (1989). *Nucleic Acids Res.* **17**, 2223–2231.

Hirao, I., Nishimura, Y., Tagawa, Y., Watanabe, K. & Miura, K. (1992). *Nucleic Acids Res.* **20**, 3891–3896.

Inman, R. B. (1964). *J. Mol. Biol.* **9**, 624–637.

Jones, T. A., Zou, J. Y., Cowan, S. W. & Kjeldgaard, M. (1991). *Acta Cryst.* A**47**, 110–119.

Kraulis, P. J. (1991). *J. Appl. Cryst.* **24**, 946–950.

Leslie, A. G. W. (1992). *Crystallographic Computing 5, From Chemistry to Biology*, edited by D. Moras, A. D. Pojarny & J.-C. Thierry. Oxford University Press.

Lu, X.-J. & Olson, W. K. (2003). *Nucleic Acids. Res.* **31**, 5108–5121.

Navaza, J. (1994). *Acta Cryst.* A**50**, 157–163.

Otwinowski, Z. & Minor, W. (1997). *Methods Enzymol.* **276**, 307–326.

Pley, H. W., Flaherty, K. M. & McKay, D. B. (1994). *Nature (London)*, **372**, 68–74.

Powell, H. R. (1999). *Acta Cryst.* D**55**, 1690–1695.

Robinson, H., van der Marel, G. A., van Boom, J. H. & Wang, A. H.-J. (1992). *Biochemistry*, **31**, 10510–10517.

Robinson, H. & Wang, A. H.-J. (1993). *Proc. Natl Acad. Sci. USA*, **90**, 5224–5228.

Rossmann, M. G. & van Beek, C. G. (1999). *Acta Cryst.* D**55**, 1631–1640.

Rupert, P. B. & Ferre-D'Amare, A. R. (2001). *Nature (London)*, **410**, 780–786.

Sakabe, N. (1991). *Nucl. Instrum. Methods Phys. Res. A*, **303**, 448–463.

Sayle, R. A. & Milner-White, E. J. (1995). *Trends Biochem. Sci.* **20**, 374–376.

Scott, W. G., Finch, J. T. & Klug, A. (1995). *Cell*, **81**, 991–1002.

Shepard, W., Cruse, W. B., Fourme, R., de La Fortelle, E. & Prangé, T. (1998). *Structure*, **6**, 849–861.

Sioud, M. (2001). *Curr. Mol. Med.* **1**, 575–588.

Steller, I., Bolotovsky, R. & Rossmann, M. G. (1997). *J. Appl. Cryst.* **30**, 1036–1040.

Sunami, T., Kondo, J., Kobuna, T., Hirao, I., Watanabe, K., Miura, K. & Takénaka, A. (2002). *Nucleic Acids Res.* **30**, 5253–5260.

Wimberly, B. T., Brodersen, D. E., Clemons, W. M. Jr Morgan-Warren, R. J., Carter, A. P., Vonrhein, C., Hartsch, T. & Ramakrishnan, V. (2000). *Nature (London)*, **407**, 327–339.

Yusupov, M. M., Yusupova, G. Z., Baucom, A., Lieberman, K., Earnest, T. N., Cate, J. H. & Noller, H. F. (2001). *Science*, **292**, 883–896.

addenda and errata

Structure of d(GCGAAAGC) (hexagonal form): a base-intercalated duplex as a stable structure. Erratum

Tomoko Sunami,[a] Jiro Kondo,[a] Ichiro Hirao,[b,c] Kimitsuna Watanabe,[d] Kin-ichiro Miura[e] and Akio Takénaka[a]*

[a]Graduate School of Bioscience and Biotechnology, Tokyo Institute of Technology, Yokohama 226-8501, Japan, [b]RIKEN GSC, Wako-shi, Saitama 351-0198, Japan, [c]Research Center for Advanced Science and Technology, University of Tokyo, Tokyo 153-8904, Japan, [d]Graduate School of Engineering, University of Tokyo, Tokyo 113-8656, Japan, and [e]Faculty of Science, Gakushuin University, Tokyo 171-8588, Japan. Correspondence e-mail: atakenak@bio.titech.ac.jp

In the paper by Sunami *et al.* [(2004), *Acta Cryst.* D**60**, 90–96] an incorrect version of Table 2 was published. The correct version is given here.

References

Lu, X.-J. & Olson, W. K. (2003). *Nucleic Acids. Res.* **31**, 5108–5121.

Shepard, W., Cruse, W. B., Fourme, R., de La Fortelle, E. & Prangé, T. (1998). *Structure*, **6**, 849–861.

Sunami, T., Kondo, J., Hirao, I., Watanabe, K., Miura, K. & Takenaka, A. (2004). *Acta Cryst.* D**60**, 90–96

Table 2
Some helical parameters and sugar puckers of the base-intercalated duplexes.

Inclin, Prop, Buckl and Open represent inclination, propeller twist, buckle and opening angles (see Lu & Olson, 2003). The C_2 residue is iodinated in 9hmt-I and brominated in 9hmt-Br. For each base pair, the upper line is for 9hmt-I, the middle line for 8hmt-h and the lower line for 9hmt-Br (Shepard *et al.*, 1998). The corresponding values for the remaining half of the duplex are omitted owing to crystallographic symmetry.

(*a*) Helical parameters.

Base pair	Inclin	Tip	Twist	dz	Prop	Buckl	Open	C1′···C1′
$G_1 \cdot C_8^*$	1	−6	26	3.1	6	−2	−3	10.7
	−2	−8	28	3.0	9	0	3	10.5
	2	3	31	3.2	6	−1	1	10.5
$C_2 : G_7^*$	6	0	55	3.3	10	13	0	10.5
	10	3	52	3.2	4	16	1	10.5
	10	0	52	3.4	8	9	−1	10.6
$G_3 : A_6^*$	†	†	†	†	−12	29	9	8.3
	†	†	†	†	−4	31	8	8.4
	†	†	†	†	−15	25	10	8.5
A form	20	0	33	2.3	12	0	−2	10.7
B form	−5	0	36	3.4	−1	0	−2	10.7

(*b*) Sugar puckers.

Nucleotide	Pucker, 9hmt-I	Pucker, 8hmt-h	Pucker, 9hmt-Br
G_1	C3′-*exo*	C3′-*exo*	C3′-*exo*
C_2	C1′-*exo*	C1′-*exo*	C1′-*exo*
G_3	C2′-*endo*	C2′-*endo*	C2′-*endo*
A_4	C3′-*endo*	C3′-*endo*	C4′-*exo*
A_5	C1′-*exo*	C1′-*exo*	C1′-*exo*
A_6	C2′-*endo*	C2′-*endo*	C2′-*endo*
G_7	C1′-*exo*	C1′-*exo*	C2′-*endo*
C_8	C2′-*endo*	C4′-*exo*	C3′-*exo*
T_9	‡	‡	‡
A form	C3′-*endo*	C3′-*endo*	C3′-*endo*
B form	C2′-*endo*	C2′-*endo*	C2′-*endo*

† A_4 and A_5 are not paired with any bases. ‡ T_9 is disordered.